
Optimization of Parameters for Quantitative Analysis of ^{123}I -Ioflupane SPECT Images for Monitoring Progression of Parkinson Disease

Phillip H. Kuo¹⁻³, Naghmehossadat Eshghi¹, Sule Tinaz⁴, Hal Blumenfeld⁴, Elan D. Louis⁴⁻⁶, and George Zubal^{4,7,8}

¹Department of Medical Imaging, Banner University Medical Center, Tucson, Arizona; ²Department of Medicine, Banner University Medical Center, Tucson, Arizona; ³Department of Biomedical Engineering, University of Arizona, Tucson, Arizona; ⁴Department of Neurology, Yale School of Medicine, New Haven, Connecticut; ⁵Department of Chronic Disease Epidemiology, Yale School of Public Health, New Haven, Connecticut; ⁶Center for Neuroepidemiology and Clinical Neurological Research, Yale School of Medicine, New Haven, Connecticut; ⁷Departments of Medical Imaging, Medicine, and Biomedical Engineering, University of Arizona Health Sciences, Tucson, Arizona; and ⁸Z-Concepts LLC, New Haven, Connecticut

Quantitative assessment of dopamine transporter imaging can aid in diagnosing Parkinson disease (PD) and assessing disease progression in the context of therapeutic trials. Previously, the software program SBRquant was applied to ^{123}I -ioflupane SPECT images acquired on healthy controls and subjects with PD. Earlier work on optimization of the parameters for differentiating between controls and subjects with dopaminergic deficits is extended here for maximizing change measurements associated with disease progression on longitudinally acquired scans. **Methods:** Serial ^{123}I -ioflupane SPECT imaging for 51 subjects with PD (conducted approximately 1 y apart) were downloaded from the Parkinson Progression Markers Initiative database. The software program SBRquant calculates the striatal binding ratio (SBR) separately for the left and right caudates and putamen regions of interest (ROIs). Parameters were varied to evaluate the number of summed transverse slices and the positioning of the striatal ROIs for determining the signal-to-noise ratio associated with their annual rate of change in SBR. The parameters yielding the largest change in the lowest putamen's SBR from scan 1 to scan 2 were determined. **Results:** From scan 1 to scan 2 in the 51 subjects, the largest annual change was observed when the putamen ROI was placed 3 pixels away from the caudate and by summing 5 central striatal slices. This resulted in an $11.2\% \pm 4.3\%$ annual decrease in the lowest putamen SBR for the group. **Conclusion:** Quantitative assessment of dopamine transporter imaging for assessing progression of PD requires specific, optimal parameters different from those for diagnostic accuracy.

Key Words: neurology; brain; ioflupane; Parkinson disease; quantitative analysis; SPECT

J Nucl Med Technol 2019; 47:70–74

DOI: 10.2967/jnmt.118.213181

Parkinson disease (PD) is the prototypical neurodegenerative disease of the nigrostriatal pathway, which extends from the substantia nigra in the midbrain to the basal ganglia. Although the clinical diagnosis of PD can be straightforward, atypical presentations and concomitant medical conditions can confound a clinical diagnosis. Therefore, dopamine transporter imaging with the widely approved radiopharmaceutical ^{123}I -ioflupane has gained acceptance for aiding in the diagnosis of PD (1–3). ^{123}I -ioflupane gained regulatory approval on the basis of visual reads, as described in the package insert for DaTscan (GE Healthcare). The associated reader study trials showed that in patients with early signs or symptoms of a parkinsonian syndrome, the positive agreement among 3 readers was 77%–79% and the negative agreement was 96% (4). Therefore, visual reads had a very high negative predictive value but had more room for improvement in positive predictive value. To aid the clinician with assessing the quantitative loss of dopaminergic transporter sites in patients, several image processing software packages have been developed over the years (5–14). Computer-aided analysis can provide critical adjunct information or a “second read,” which may be particularly useful for challenging cases (15–17).

Decades of study of this disease have led to clinical trials with specific therapeutic interventions using indirect and direct dopaminergic agonists (18). Proper enrollment into clinical trials requires reliable, accurate diagnosis. Beyond diagnosis, dopamine transporter imaging has tremendous research potential for monitoring response to disease-modifying therapies; however, ioflupane is not approved for following progression of disease or response to therapies. Imaging markers of presynaptic dopaminergic function may offer an objective biomarker of the level of neuronal degeneration. In studies of PD patients, manual analyses of scans of presynaptic dopamine radioligands revealed decreases in radiotracer uptake in the range of 4%–11% per year by serial imaging over 1–4 y (19). These relatively

Received Apr. 19, 2018; revision accepted Aug. 14, 2018.
For correspondence or reprints contact: Naghmehossadat Eshghi, Department of Medical Imaging, Banner University Medical Center, 1501 N. Campbell Ave., P.O. Box 245067, Tucson, AZ 85724.
E-mail: neshghi@radiology.arizona.edu
Published online Aug. 23, 2018.
COPYRIGHT © 2019 by the Society of Nuclear Medicine and Molecular Imaging.

small annual changes in combination with high intersubject variability from both biologic and technical sources mandate the need for automated quantification for reproducible analyses.

The Parkinson Progressive Marker Initiative (PPMI) is a large, international, multicenter clinical study to identify a variety of biomarkers for progression of de novo PD. Dopamine transporter imaging with ^{123}I -ioflupane is an important biomarker under study in this trial. A software program must handle scans from a variety of clinical sites, and therefore, the database of PPMI is an excellent dataset to test the robustness of software analysis. Optimized software quantitation using this extensive database can serve as a valuable tool for evaluating disease progression, which would otherwise be a challenging task for visual reads.

MATERIALS AND METHODS

Subject Population

Previously, a cohort of 336 subjects (215 PD patients and 121 healthy controls) scanned with ^{123}I -ioflupane was downloaded from the PPMI database (<http://www.ppmi-info.org/>). The PPMI SPECT data were reconstructed from the site-specific projection data using the site-specific attenuation corrections. Each brain volume was spatially normalized to a standard geometry. Results and parameters for optimal sensitivity and specificity for diagnosis of PD were reported (20). Of this cohort, 51 PD subjects had 1-y longitudinal follow-up scans, which were used for this study.

SBRquant Automated Image Processing Steps

The fully automated SBRquant software package builds on the algorithms described in previous developments (13,21–25). The analysis scripts were developed using MATLAB, version 2012a (MathWorks), resulting in a fully automated Microsoft Windows 7-executable program that carries out the image processing steps.

In the first step, locating the central slice, the central plane through the subject's striatum is found by locating the maximum value in the "top-to-bottom" profile in the summed sagittal view of the reconstructed images.

The second step is summing the central striatal slices. To maintain symmetry above and below the central slice for analysis, a parameter N describes the number of slices that are summed to place the 2-dimensional regions of interest (ROIs). The same number of slices is added above and below the central slice through the striatum; hence, the total slices summed for quantitative analysis is always an odd number N as shown in Figure 1.

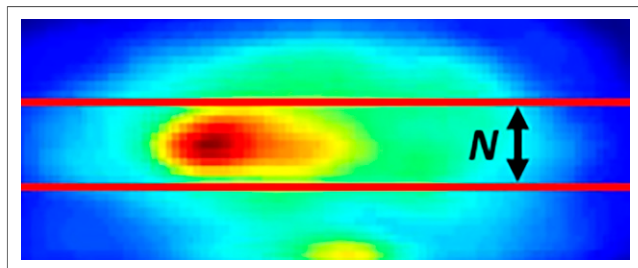


FIGURE 1. Summed sagittal slices of brain volume showing selection of transverse slices (between red lines); total slices added for analysis is N .

In the third step, locating the individual striata, the intensity centroids of the left and right caudates are located within the 2-dimensional transverse summed slice by looking for maxima in the subject's left-to-right profiles.

In the fourth step, placing the ROI, a crescent-shaped ROI is placed on the occipital area of the brain. A caudate ROI (green circle) is moved within the vicinity of each located striatum until SBRquant locates a maximum count value (representing the initial location of each caudate); the smaller caudate ROI (white circle) is placed in its center and is used for the caudate count density measurement.

In the fifth step, locating the left and right putamina, the distance from the caudate white ROI to the putamen white ROI is selected using the parameter d in units of pixels (Fig. 2) and allows placement of the ROI over the putamen to be varied individually for all subjects in the group being analyzed. Fixing the distance to the caudate, the putamen ROI is moved to different angular positions around the caudate until a maximum value is found for extracting the putamen count density.

In the final step, calculating the specific striatal binding ratio (SBR), the SBR in each scan is calculated as the background-subtracted ratio of the caudate or putamen count density to the occipital ROI count density (whereby the occipital ROI is used to calculate the background). A final report is generated with all quantitative values written into the image containing the ROI placements (Fig. 2).

Optimizing the Parameters for Annual Change

For the 51 PD subjects who had a second scan approximately 1 y later, a rate of change per year in the lowest putamen SBR was evaluated by varying the number of summed transverse slice (N) and the separation between the caudate and putamen ROIs (d) (Figs. 1 and 2). The parameters yielding the largest change per year of SBR from scan 1 to scan 2 were determined.

RESULTS

The resulting annual change for the 51 subjects in this study is shown as a function of N and d (Fig. 3). Because fractional change is plotted as negative values (decreases with time), the strongest changes are seen lowest in the graph. The annual changes are graphed for 4 parameters (lowest putamen, average of putamina, average of caudates, and average of all caudates and putamina). Of these parameters, the change in the lowest putamen SBR yields the largest average annual change, with a fractional change of 0.112 (11.2%). This most significant change occurred with the parameters $N = 11$ and $d = 3$.

DISCUSSION

The previously published analysis of 336 subjects (215 PD patients, 121 healthy controls) yielded a sensitivity and specificity of 95.8% and 98.3% for the diagnosis of PD (20). The systematic evaluation for the optimal parameters for that given dataset resulted in selecting parameters $N = 9$ and $d = 8$ (where N is the number of summed slices and d is the number of pixels from the caudate ROI to the putamen ROI). When analyzing 51 subjects with serial scans, a largest $11.2\% \pm 4.3\%$ annual change was calculated using the same method as for finding optimized analysis parameters, but with the parameters $N = 11$ and $d = 3$.

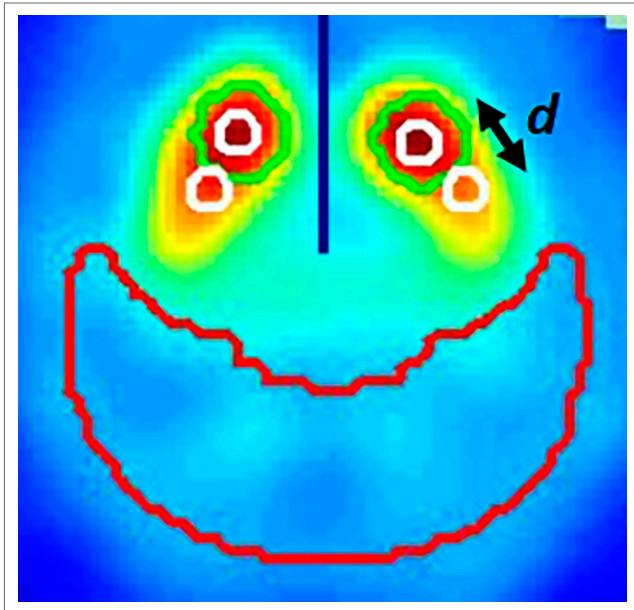


FIGURE 2. Summed transverse slices of brain volume showing ROI placements (white circles) for calculating SBRs. Distance between caudate and putamen ROIs is d , measured in pixels. Black line is automated location of center line between left and right striata. Green circle is SBRquant initial location of left and right caudates and is used to place ROIs onto center of caudate; putamen ROI is placed relative to caudate ROI. Reference ROI is red crescent in occipital region.

The optimal threshold of the SBR of the lowest putamen for discriminating between PD patients and healthy controls in the optimization study of 336 subjects was 1.037. The sensitivity and specificity of the quantitative discrimination method described here is determined primarily by selection of summed slices and positioning of ROIs that yield a quantitative number.

An advantage of analyzing the SPECT scans using the methods described here is that the accuracy and reproducibility of the quantitative measures do not rely on the registration of the individual subject's scan to the normalizing template. The normalization of each individual scan to a standard geometry template is used primarily to align all the scans into a consistent orientation, resulting in a uniform size and number of slices for each scan. The placement of the caudate and putamen ROI is independent of the registration accuracy to the template. The placement of the ROIs relies primarily on algorithms that locate the structures in the brain and place the ROIs according to predetermined local characteristics of the target structures. In PD, the decrease in radiotracer uptake in the striatum per annum is small and therefore difficult to follow visually. Objective quantitation of striatal binding is therefore crucial for detecting changes in sequential imaging for response to therapies. To our knowledge, this study is the first to demonstrate that different algorithmic parameters are necessary for optimal analysis of the initial scan for diagnosis versus serial imaging for progression of disease. With severity and

progression of disease, the activity in the putamen decreases, and visually, the putamen becomes shorter, with greater loss of activity from posterior to anterior with time. Since the putamen shortens with disease progression, using an ROI placement optimal for discriminating healthy controls from PD patients would result in a smaller and less reproducible percentage change. To detect a larger, more reproducible percentage change, the ROI needs to be moved closer to the caudate, where disease progression has a larger effect on the radiotracer uptake. Hence, we note that the parameters yielding the best discrimination between PD subjects and healthy controls are different from the parameters yielding the largest annual change calculated from 2 scans obtained approximately 1 y apart. This seems reasonable since differentiating between PD patients and healthy controls would rely on quantitating the uptake in the more posterior aspect of the putamen (putamen ROI position at $d = 8$), whereas changes in disease progression would be more strongly noted anteriorly, closer to the caudate (putamen ROI position at $d = 3$). It is further interesting to note that for differentiating between PD patients and healthy controls, fewer slices need to be summed ($N = 9$; i.e., 9 slices summed for analysis) to optimize the area-under-the-curve measurement than would be required to calculate the largest change between annual scans ($N = 11$; i.e., 11 slices summed for analysis); this may

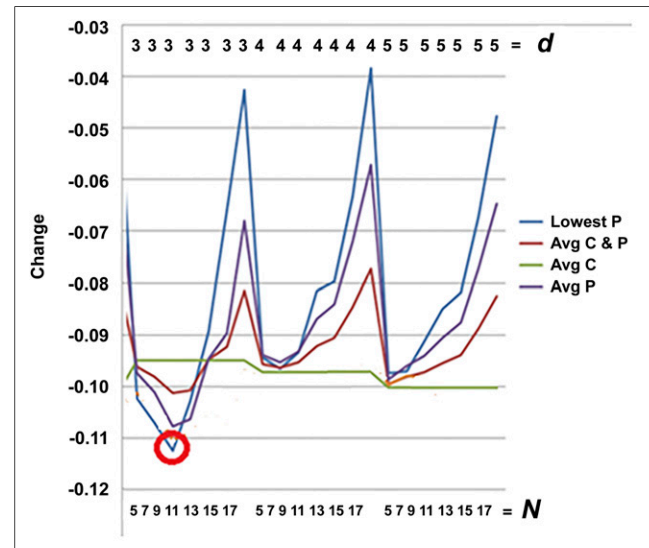


FIGURE 3. Average annual change between repeat scans for 51 subjects is plotted on y-axis as function of 2 parameters: distance in pixels between caudate and putamen ROIs, d , on upper x-axis and number of central striatal summed transverse slices, N , on lower x-axis. Average annual changes are graphed for 4 parameters: lowest putamen (Lowest P), average of both caudates and putamina (Avg C & P), average of caudates (Avg C), and average of putamina (Avg P). Largest average annual change (red circle) is obtained with lowest putamen parameter when summing 11 transverse slices ($N = 11$) and placing putamen ROI 3 pixels from caudate ROI ($d = 3$). Largest average annual change for group was fractional change of 0.112 (11.2%).

be due to the convoluted geometry of the putamen, so that more summed slices would ensure that the structure is fully sampled by the 2-dimensional ROI.

These factors lead us to an additional consideration. There is indeed no singular best method for calculating SBR, in that the ROI placements on the caudate and especially the putamen strongly influence the calculated SBR. One could argue that either averaging the uptake over the complete anatomic structure of the putamen or selecting the highest remaining uptake in either the anterior or the posterior region of the putamen could be the best measure for quantitating the ^{123}I -ioflupane SPECT scan. Each of these 3 samples of the putamen will return quite different measures of uptake. Selecting 1 of these 3 possible quantitation measures depends directly on which aspect of the disease we intend to evaluate. Additionally, the background reference region (usually placed on the occipital lobe) represents low (relatively noisy) uptake values, is used as the divisor in calculating the SBR, and strongly influences the resulting SBR values. This leads us to the usual trade-off between accuracy and precision whereby consistent, reproducible (automated) analyses may have an advantage over manual methods, since differences between analysis sites and even analysts can introduce variability into the quantitative results.

Since no operator intervention is required, the reproducibility of reanalyzed data exhibits no operator variability when using SBRquant. The fully automated nature of the program (and the processing time of approximately 40 s per scan) would ease implementation of the analysis into the daily clinical workflow of the technologist or physician. This software is derived from and tested on the PPMI database, which has scans from numerous sites and countries; therefore, the program has the robustness to accommodate different imaging techniques from a spectrum of imaging centers and γ -cameras.

A potential limitation of the study is the cohort size ($n = 51$). These 51 patients do not necessarily represent an accurate sampling of the range of patients with PD. Given a larger group of subjects, variations in the annual loss of radiotracer binding could be determined with better accuracy and precision. Future work should include further optimizing these parameters in larger cohorts when available. These parameters may also be assessed for different clinical settings and different racial or ethnic groups.

These developments enhance the clinical power of imaging studies in that they reduce the variability of quantitative results obtained between image-processing technologists and image-analysis sites. This further helps to reduce the number of subjects who need to be studied for investigating new diagnostic and therapeutic agents, as well as to deliver more consistent and reproducible clinical evaluations.

CONCLUSION

SBRquant, a fully automated software for quantitative analysis of ^{123}I -ioflupane SPECT scans, was previously optimized for diagnosis of PD and, in this study, has been

optimized for measuring progression in PD. The optimal parameters (number of summed transverse slices and distance between putamen and caudate ROI) have now been determined independently for discriminating PD patients from healthy controls, as well as for evaluating percentage change per annum between serial scans.

DISCLOSURE

Phillip Kuo is a consultant for inviCRO and a consultant and speaker for GE Healthcare. George Zubal is owner of Z-Concepts LLC. Phillip Kuo has received support as a consultant, investigator, or speaker for Genentech, GE Healthcare, inviCRO, Lilly, Merck, MD Training @Home, Molecular Neuroimaging Institute, and Navidea. George Zubal has received support from the National Institutes of Health (NIH): STTR phase II renewal (5R42NS055475-06, principal investigator), SBIR FastTrack (NS055475, principal investigator), and from the Department of Energy (DOE): SBIR phase I (83229S07-I, principal investigator). This work was supported by the following grants: NIH STTR phase II renewal (5R42NS055475), NIH SBIR FastTrack (NS055475), and DOE SBIR phase I (83229S07-I). Data used in the preparation of this article were obtained from the Parkinson's Progression Markers Initiative database (www.ppmi-info.org/data). For up-to-date information on the study, visit www.ppmi-info.org/data. The Parkinson's Progression Markers Initiative, a public-private partnership, is funded by the Michael J. Fox Foundation for Parkinson's Research and funding partners, including Abbott, Abbvie, Avid, Biogen Idec, Bristol-Myers Squibb, Covance, GE Healthcare, Genentech, GlaxoSmithKline, Lilly, Lundbeck, Merck, Meso Scale Discovery, Pfizer, Piramal, Roche, Sanofi Genzyme, Servier, Takeda, Teva, UCB, and Golub Capital. No other potential conflict of interest relevant to this article was reported.

REFERENCES

1. Tatsch K, Poeppel G. Nigrostriatal dopamine terminal imaging with dopamine transporter SPECT: an update. *J Nucl Med*. 2013;54:1331-1338.
2. Catafau AM, Tolosa E. Impact of dopamine transporter SPECT using ^{123}I -ioflupane on diagnosis and management of patients with clinically uncertain Parkinsonian syndromes. *Mov Disord*. 2004;19:1175-1182.
3. Ichise M, Kim YJ, Ballinger JR, et al. SPECT imaging of pre- and postsynaptic dopaminergic alterations in L-dopa-untreated PD. *Neurology*. 1999;52:1206-1214.
4. Marshall VL, Reiningner CB, Marquardt M, et al. Parkinson's disease is overdiagnosed clinically at baseline in diagnostically uncertain cases: a 3-year European multicenter study with repeat [^{123}I]FP-CIT SPECT. *Mov Disord*. 2009;24:500-508.
5. Benítez-Rivero S, Marin-Oyaga VA, Garcia-Solis D, et al. Clinical features and ^{123}I -FP-CIT SPECT imaging in vascular parkinsonism and Parkinson's disease. *J Neurol Neurosurg Psychiatry*. 2013;84:122-129.
6. Ciarmiello A, Giovacchini G, Guidotti C, et al. Weighted registration of ^{123}I -FP-CIT SPECT images improves accuracy of binding potential estimates in pathologically low striatal uptake. *J Cell Physiol*. 2013;228:2086-2094.
7. Duchesne S, Rolland Y, Verin M. Automated computer differential classification in Parkinsonian syndromes via pattern analysis on MRI. *Acad Radiol*. 2009;16:61-70.
8. Lee JD, Huang CH, Weng YH, Lin KJ, Chen CT. Improved accuracy of brain MRI/SPECT registration using a two-cluster SPECT normalization algorithm and a combinative similarity measure: application to the evaluation of Parkinson's disease. *Ann Nucl Med*. 2007;21:197-207.

9. Pereira JB, Ibarretxe-Bilbao N, Marti MJ, et al. Assessment of cortical degeneration in patients with Parkinson's disease by voxel-based morphometry, cortical folding, and cortical thickness. *Hum Brain Mapp.* 2012;33:2521–2534.
10. Skanjeti A, Angusti T, Iudicello M, et al. Assessing the accuracy and reproducibility of computer-assisted analysis of ^{123}I -FP-CIT SPECT using BasGan (V2). *J Neuroimaging.* 2014;24:257–265.
11. Söderlund TA, Dickson JC, Prvulovich E, et al. Value of semiquantitative analysis for clinical reporting of ^{123}I -2-beta-carbomethoxy-3beta-(4-iodophenyl)-N-(3-fluoropropyl) nortropane SPECT studies. *J Nucl Med.* 2013;54:714–722.
12. Varrone A, Dickson JC, Tossici-Bolt L, et al. European multicentre database of healthy controls for [^{123}I]FP-CIT SPECT (ENC-DAT): age-related effects, gender differences and evaluation of different methods of analysis. *Eur J Nucl Med Mol Imaging.* 2013;40:213–227.
13. Zubal IG, Early M, Yuan O, Jennings D, Marek K, Seibyl JP. Optimized, automated striatal uptake analysis applied to SPECT brain scans of Parkinson's disease patients. *J Nucl Med.* 2007;48:857–864.
14. Morton RJ, Guy MJ, Clauss R, Hinton PJ, Marshall CA, Clarke EA. Comparison of different methods of DatSCAN quantification. *Nucl Med Commun.* 2005;26:1139–1146.
15. Kuo PH, Avery R, Krupinski E, et al. Receiver-operating-characteristic analysis of an automated program for analyzing striatal uptake of ^{123}I -ioflupane SPECT images: calibration using visual reads. *J Nucl Med Technol.* 2013;41:26–31.
16. Kuo PH, Lei HH, Avery R, et al. Evaluation of an objective striatal analysis program for determining laterality in uptake of ^{123}I -ioflupane SPECT images: comparison to clinical symptoms and to visual reads. *J Nucl Med Technol.* 2014;42:105–108.
17. Booi J, Dubroff J, Pryma D, et al. Diagnostic performance of the visual reading of ^{123}I -ioflupane SPECT images with or without quantification in patients with movement disorders or dementia. *J Nucl Med.* 2017;58:1821–1826.
18. Seibyl JP. Imaging studies in movement disorders. *Semin Nucl Med.* 2003;33:105–113.
19. Seibyl JP. Single-photon emission computed tomography and positron emission tomography evaluations of patients with central motor disorders. *Semin Nucl Med.* 2008;38:274–286.
20. Tinaz S, Chow C, Kuo PH, et al. Semiquantitative analysis of dopamine transporter scans in patients with Parkinson disease. *Clin Nucl Med.* 2018;43:e1–e7.
21. Booi J, de Jong J, de Bruin K, Knol R, De Win MM, van Eck-smit BL. Quantification of striatal dopamine transporters with ^{123}I -FP-CIT SPECT is influenced by the selective serotonin reuptake inhibitor paroxetine: a double-blind, placebo-controlled, crossover study in healthy control subjects. *J Nucl Med.* 2007;48:359–366.
22. Filippi L, Manni C, Pierantozzi M, et al. ^{123}I -FP-CIT semi-quantitative SPECT detects preclinical bilateral dopaminergic deficit in early Parkinson's disease with unilateral symptoms. *Nucl Med Commun.* 2005;26:421–426.
23. Germano G, Kavanagh PB, Su HT, et al. Automatic reorientation of three-dimensional, transaxial myocardial perfusion SPECT images. *J Nucl Med.* 1995;36:1107–1114.
24. Tatsch K, Poepperl G. Quantitative approaches to dopaminergic brain imaging. *Q J Nucl Med Mol Imaging.* 2012;56:27–38.
25. Tossici-Bolt L, Hoffmann SM, Kemp PM, Mehta RL, Fleming JS. Quantification of [^{123}I]FP-CIT SPECT brain images: an accurate technique for measurement of the specific binding ratio. *Eur J Nucl Med Mol Imaging.* 2006;33:1491–1499.